

How flexible is the disulfide linker? A combined rotational-computational investigation of diallyl disulfide

Jean Demaison,^{*a} Natalja Vogt,^{a,b} Rizalina Tama Saragi,^c Marcos Juanes,^c
Heinz Dieter Rudolph,^a Alberto Lesarri^{*c}

^a Section of Chemical Information Systems, University of Ulm, 89069 Ulm (Germany), E-mail: jean.demaison@gmail.com

^b Department of Chemistry, Lomonosov Moscow State University, 119992 Moscow (Russia)

^c Departamento de Química Física y Química Inorgánica – IU CINQUIMA, Facultad de Ciencias, Universidad de Valladolid, 47011 Valladolid (Spain). E-mail: lesarri@qf.uva.es, Web: www.uva.es/lesarri

Experimental methods

The rotational spectrum of diallyl disulfide was recorded with a chirped-pulsed Fourier transform microwave spectrometer (2-8 GHz), following Pate's design.¹ A commercial sample of diallyl disulfide, which is liquid at room temperature, was located in a cylindrical reservoir inserted in the carrier gas line, external to the expansion chamber. The sample expanded near-adiabatically at room temperature through a pulsed (solenoid-driven) injection valve into the evacuated chamber. Neon at stagnation pressures of 1.5 bar was used as carrier gas, using a circular nozzle with a diameter of 0.5 mm. The supersonic jet was probed with a microwave chirped pulse, recording the resulting transient molecular emission in the time domain. In this experiment an excitation pulse of 4 μ s created by an arbitrary waveform generator was amplified to 20 W and radiated through a horn antenna, perpendicular to the propagation of the jet expansion. A molecular transient emission (spanning 40 μ s) was detected through a second collinear horn, recorded with a digital oscilloscope and Fourier-transformed to produce the frequency domain spectrum. Five excitation cycles were used per gas pulse. Typical linewidths of the rotational transitions (FWHM) reach ca. 100 kHz. All frequency oscillators are locked to a rubidium standard, providing frequency accuracies below 5 kHz.

Computational methods

1. *Electronic structure models*

Three distinct levels of electronic structure theory have been used in this study: second-order Møller–Plesset perturbation theory (MP2),² coupled cluster theory including single and double excitations (CCSD)³ augmented with a perturbational estimate of the effects of connected triple excitations, CCSD(T),⁴ and Kohn–Sham density functional theory (DFT)⁵ using Becke's three-parameter hybrid exchange functional⁶ and the Lee–Yang–Parr correlation functional,⁷ together denoted as B3LYP.

For the CCSD(T) and MP2 electronic structure computations several basis sets were employed: (a) the correlation-consistent polarized triple-zeta, and quadruple-zeta basis sets, cc-pVTZ, and cc-pVQZ⁸ which are abbreviated as VTZ, and VQZ, respectively, throughout this paper. For the sulfur atom, an extra hard d function is added to take into account innershell polarization effects in the case of second-row atoms, i.e. the V(T+d)Z and V(Q+d)Z basis sets were used;⁹ (b) the correlation-consistent polarized weighted core-valence triple zeta and quadruple zeta basis sets (abbreviated here as wCVTZ and wCVQZ, respectively)^{10,11,12} which are used to improve the computed structure by the inclusion of core correlation effects.¹³

B3LYP computations were performed with the split-valence basis set 6-311++G(d,p). Grimme's empirical dispersion was added with Becke-Johnson damping (D(3)-BJ).¹⁴

The frozen-core approximation (hereafter denoted as FC), *i.e.*, keeping the core orbitals of the second-row atoms doubly occupied during correlated-level calculations, was used at the MP2 and CCSD(T) levels, and all-electron (AE) MP2/wCVTZ and CCSD(T)/wCVTZ as well as MP2/wCVQZ computations were also performed to gauge the effect of core correlation on the structural parameters. In order to estimate the rovibrational corrections to the experimental ground-state rotational constants, the anharmonic force fields up to semidiagonal quartic terms¹⁵ were calculated for each isotopologue at the MP2_FC/cc-pV(T+d)Z level.

The MP2 and DFT calculations were performed with the Gaussian 09 (Release C.01) package¹⁶ whereas the MolPro program¹⁷ was used for the CCSD(T) calculations

2. *Calculation of the predicate observations*

Briefly, the MP2/VTZ level of theory supplies an accurate prediction for the C–H lengths as well as for the C–C single bond lengths. The accuracy is about 0.002 Å for the C–H bonds and slightly better than 0.003 Å for the C(sp³)-C(sp³) bond lengths. For the bond angles, the mean accuracy is 0.4° for the MP2/VTZ level of theory and 0.25° for the MP2/VQZ level. In many cases, the difference between the MP2/VTZ and the MP2/VQZ angles is small. It is particularly true for the $\angle(\text{HCH})$ and $\angle(\text{CCH})$ angles. Note that the bond angles may be obtained with an accuracy better than 0.4° using the 6-311+G(3df,2pd) basis set instead of the VTZ one.

For DADS we need a prediction of the S-S, C-S, C=C and C(sp²)-C(sp³) bond lengths. The case of the S-S and C-S bonds has been discussed previously,¹⁸ and it appears that the MP2/V(T+d)Z values are close to the equilibrium ones. The case of the double bond C=C is easy. A list of values is given in Table S18 below. Because its range is rather small, 0.028 Å, it is possible to assume as a first approximation that the offset $r_e - r(\text{MP2/cc-pVTZ})$ is constant. The value found is -0.028(12) Å.

The case of the C(sp²)-C(sp³) bond length is more complicated. When the bond is a true single bond as in ethane, there is no significant difference between the r_e value and the MP2/VTZ value.¹⁹ However, when the CC bond shortens, the MP2/VTZ method slightly overestimate the length but there is a correlation between the r_e value and the difference $r_e - r[\text{MP2/VTZ}]$, the value of the correlation coefficient being -0.85. Although the scattering of data is significant, it is possible to estimate that the C-C bond

lengths of DADS computed at the MP2/VTZ level are too large by about 0.0011 Å with a standard deviation of 0.0012 Å.

The case of the dihedral angles is more difficult because it is established that the MP2 method fails to deliver accurate dihedral angles, the error being sometimes as large as several degrees.²⁰ However, as shown in Ref. 18, it is possible to determine accurate dihedral angles using the rotational constants (even with a very approximate rovibrational correction). This is expected to give good results for the dihedral angles $\tau(\text{CSSC})$ and $\tau(\text{SCCC})$. However, the $\tau(\text{HCCX})$ dihedral angles, with X = C, or S, will remain close to their predicate values because there is no isotopic substitution available for the hydrogen atoms. Recently, an approximate formula to estimate the dihedral angles has been proposed²⁰

$$\begin{aligned} \tau_e - \tau [\text{MP2_FC/cc-pVTZ}] = \\ -0.296(15) \times ([\text{MP2_FC/cc-pVTZ}] - \tau[\text{B3LYP/6-311+G(3df,2pd)}]) \end{aligned} \quad (1)$$

and was used in this work. The details of the calculations are given in Table S13-S14.

In conclusion, at the MP2/cc-pV(T+d)Z level of theory, it seems possible to determine the equilibrium structure of DADS with an accuracy better than 0.003 Å for the bond lengths and 0.4° for the bond angles. Indeed, comparison with the r_e^{BO} parameters of Table 2 and S13-S14 gives a median absolute deviation (MAD) of 0.0004 Å for the bond lengths, the mean absolute deviation being 0.0010 Å, and the maximum deviation being 0.0053 Å for the S-S bond. For the bond angles, these values are: 0.20°; 0.20° and 0.53° for the $\angle(\text{S'C1'C24})$ angle, respectively. Inspection of Table S13-S14 indicates that the torsional angles are predicted with a standard deviation of 0.7°.

REFERENCES

- ¹ a) S. T. Shipman, B. H. Pate, in *Handbook of High Resolution Spectroscopy*, ed. M. Quack and F. Merkt, Wiley, New York, 2011, pp. 801–828. b) C. Pérez, S. Lobsiger, N. A. Seifert, D. P. Zaleski, B. Temelso, G. C. Shields, Z. Kisiel, B. H. Pate, *Chem. Phys. Lett.* 2013, **571**, 1-15.
- ² C. Møller, M. S. Plesset, *Phys. Rev.* 1934, **46**, 618–622.
- ³ G. D. Purvis, R. J. Bartlett, *J. Chem. Phys.* 1982, **76**, 1910–1918.
- ⁴ K. Raghavachari, G. W. Trucks, J. A. Pople, M. A. Head-Gordon, *Chem. Phys. Lett.* 1989, **157**, 479–483.
- ⁵ W. Kohn, L. J. Sham, *Phys. Rev. A* 1965, **140**, 1133–1138.
- ⁶ A. D. Becke, *J. Chem. Phys.* 1993, **98**, 5648–5652.
- ⁷ C. T. Lee, W. T. Yang, R. G. Parr, *Phys. Rev. B* 1988, **37**, 785–789.
- ⁸ T. H. Dunning, Jr. *J. Chem. Phys.* 1989, **90**, 1007-1023.
- ⁹ T. H. Dunning, Jr., K. A. Peterson, A. K. Wilson, *J. Chem. Phys.* 2001, **114**, 9244-9253.
- ¹⁰ D. E. Woon, T. H. Dunning, Jr. *J. Chem. Phys.* 1995, **103**, 4572–4585.
- ¹¹ K. A. Peterson, T. H. Dunning, Jr. *J. Chem. Phys.* 2002, **117**, 10548–10560.
- ¹² Basis sets were obtained from the Extensible Computational Chemistry Environment Basis Set Database, Version 6/19/03, as developed and distributed by the Molecular Science Computing Facility, Environmental and Molecular Sciences Laboratory which is part of the Pacific Northwest Laboratory, P.O. Box 999, Richland, Washington 99352, USA, and funded by the U.S. Department of Energy. The Pacific Northwest Laboratory is a multi-program laboratory operated by Battelle Memorial Institute for the U.S. Department of Energy under contract DE-AC06-76RLO 1830. Contact David Feller or Karen Schuchardt for further information.
- ¹³ A. G. Császár, W. D. Allen, *J. Chem. Phys.* 1996, **104**, 2746–2748.
- ¹⁴ S. Grimme, S. Ehrlich, L. Goerick, *J. Comp. Chem.* 2011, **32**, 1456-1465.
- ¹⁵ A. G. Császár, Anharmonic Molecular Force Fields. *WIREs Comput. Mol. Sci.* 2012, **2**, 273–289.
- ¹⁶ M. J. Frisch, G. W. Trucks, H. B. Schlegel, G. E. Scuseria, M. A. Robb, J. R. Cheeseman, G. Scalmani, V. Barone, G. A. Petersson, H. Nakatsuji, X. Li, M. Caricato, A. Marenich, J. Bloino, B. G. Janesko, R. Gomperts, B. Mennucci, H. P. Hratchian, J. V. Ortiz, A. F. Izmaylov, J. L. Sonnenberg, D. Williams-Young, F. Ding, F. Lipparini, F. Egidi, J. Goings, B. Peng, A. Petrone, T. Henderson, D. Ranasinghe, V. G. Zakrzewski, J. Gao, N. Rega, G. Zheng, W. Liang, M. Hada, M. Ehara, K. Toyota, R. Fukuda, J. Hasegawa, M. Ishida, T. Nakajima, Y. Honda, O. Kitao, H. Nakai, T. Vreven, K. Throssell, J. A. Montgomery, Jr., J. E. Peralta, F. Ogliaro, M. Bearpark, J. J. Heyd, E. Brothers, K. N. Kudin, V. N. Staroverov, T. Keith, R. Kobayashi, J. Normand, K. Raghavachari, A. Rendell, J. C. Burant, S. S. Iyengar, J. Tomasi, M. Cossi, J. M. Millam, M. Klene, C. Adamo, R. Cammi, J. W. Ochterski, R. L. Martin, K. Morokuma, O. Farkas, J. B. Foresman, and D. J. Fox, Gaussian 09, Revision C.01; Gaussian, Inc., Wallingford, CT, 2009.
- ¹⁷ a) H.-J. Werner, P. J. Knowles G. Knizia, F. R. Manby, M. Schütz, *WIREs Comput. Mol. Sci.* 2012, **2**, 242. b) H.-J. Werner, P. J. Knowles, R. Lindh, F. R. Manby, M. Schütz, P. Celani, T. Korona, A. Mitrushenkov, G. Rauhut, T. B. Adler, R. D. Amos, A. Bernhardsson, A. Berning, D. L. Cooper, M. J. O. Deegan, A. J. Dobbyn, F. Eckert, E. Goll, C. Hampel, G. Hetzer, T. Hrenar, G. Knizia, C. Köpli, Y. Liu, A. W. Lloyd, R. A. Mata, A. J. May, S. J. McNicholas, W. Meyer, M. E. Mura, A. Nicklass, P. Palmieri, K. Pflüger, R. Pitzer, M. Reiher, U. Schumann, H. Stoll, A. J. Stone, R. Tarroni, T. Thorsteinsson, M. Wang and A. Wolf, MOLPRO, 2009.
- ¹⁸ J. Demaison, N. Vogt, R. T. Saragi, M. Juanes, H. D. Rudolph, A. Lesarri, *ChemPhysChem*, 2019, **20**, 366
- ¹⁹ J. Demaison, N. C. Craig, E. J. Cocinero, J.-U. Grabow, A. Lesarri, H. D. Rudolph, *J. Phys. Chem. A* 2012, **116**, 8684-8692.
- ²⁰ M. Juanes, N. Vogt, J. Demaison, I. León, A. Lesarri, H. D. Rudolph, *Phys. Chem. Chem. Phys.* 2017, **19**, 29162-29169.

Figure S1. Rotatable 3D molecular model of the most stable isomer 1 of DADS (C_I).

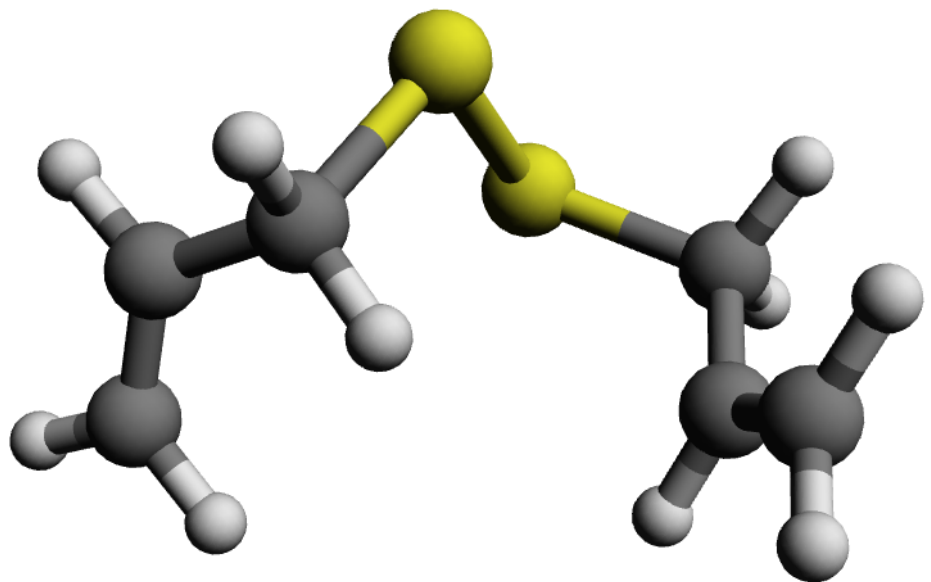


Figure S2. Rotatable 3D molecular model of the C_2 -symmetric second most stable isomer 2 of DADS.

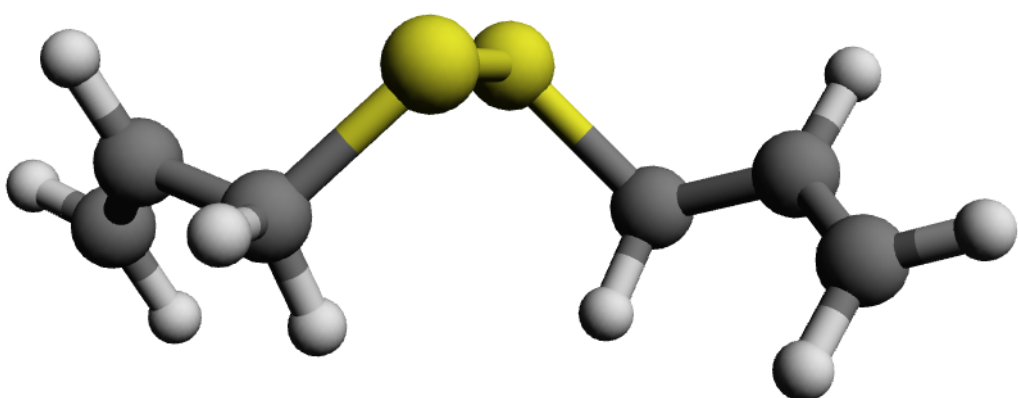


Figure S3. A section of the microwave spectrum of DADS, showing the different monosubstituted species for the bR rotational transition $J_{K_{-1},K_{+1}} = 2_{2,1} \leftarrow 1_{1,0}$. Each atomic position produces a different isotopic spectrum according to natural abundance, confirming a C_1 structure. The two ${}^{34}\text{S}$ transitions are expanded in the lower trace.

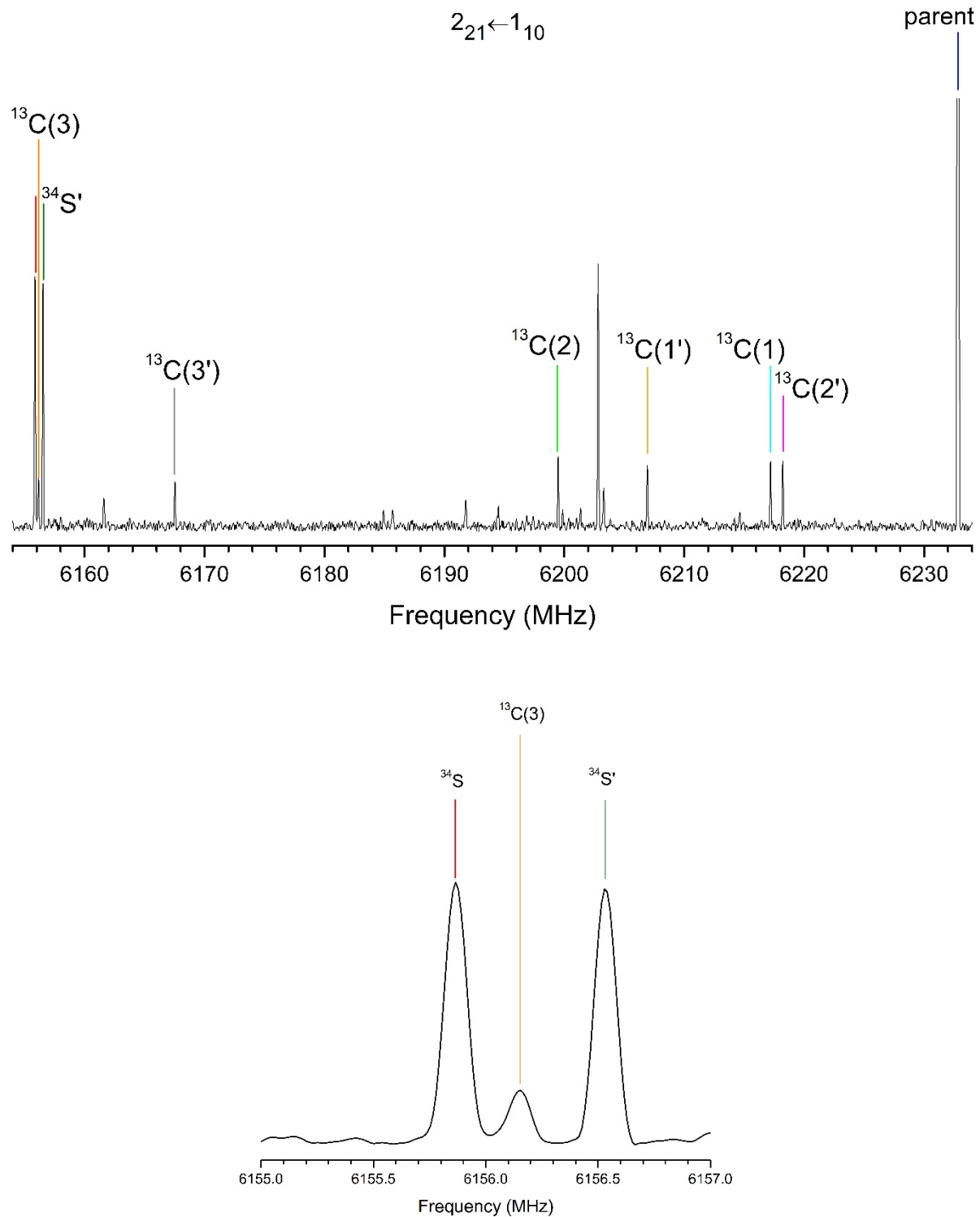


Table S1. Conformational search of diallyl disulfide (B3LYP-D3(BJ)/6-311++G(d,p)), with indication of the molecular symmetry.

	Conformer 1	Conformer 2 (C_2 symmetry)	Conformer 3	Conformer 4	Conformer 5	Conformer 6 (C_2 symmetry)
A / MHz ^a	1749.42	2486.46	2065.09	2057.91	2123.21	1477.06
B / MHz	972.75	785.75	888.91	891.87	827.93	1260.08
C / MHz	877.24	725.98	679.03	679.81	719.17	897.29
κ	-0.781	-0.932	-0.697	-0.692	-0.845	0.252
D_J / kHz	0.57	0.45	0.43	0.42	0.20	0.60
D_{JK} / kHz	-1.78	-4.44	1.94	1.79	-0.51	-0.84
D_K / kHz	3.6	16.3	0.32	0.47	3.3	0.57
d_I / kHz	-0.12	0.02	-0.18	-0.17	-0.02	0.08
d_2 / kHz	-0.01	0.00	-0.05	-0.05	0.00	0.05
μ_a / D	-0.6	0.0	0.0	0.0	0.7	0.0
μ_b / D	-1.8	0.0	1.9	1.9	1.8	-1.7
μ_c / D	0.0	1.8	0.6	0.6	-0.5	0.0
μ_{TOTAL} / D	1.9	1.8	2.0	2.0	2.0	1.7
ΔE / kJ mol ⁻¹ ^b	0.0	3.0	3.3	3.3	3.4	3.5
ΔG / kJ mol ⁻¹	0.0	1.7	1.8	1.9	3.2	4.3

^aRotational constants (A , B , C), asymmetry parameter (κ), Watson's S-reduction centrifugal distortion constants (D_J , D_{JK} , D_K , d_I , d_2) and electric dipole moments (μ_α , $\alpha = a, b, c$). ^bRelative energies corrected with the zero-point contributions (ΔE) and Gibbs energy (ΔG , 298K, 1 atm).

Table S2. Rotational transitions for the parent species of DADS.

	J'	K_{-I}'	K_{+I}'	J''	K_{-I}''	K_{+I}''	Freq. ^a (MHz)	o-c ^b (MHz)
1	6	2	4	6	1	5	2136.4691	-0.0029
2	5	2	3	5	1	4	2137.4588	0.0026
3	4	2	2	4	1	3	2204.3717	-0.0018
4	7	2	5	7	1	6	2224.6889	-0.0012
5	3	2	1	3	1	2	2308.4525	0.0032
6	6	1	5	6	0	6	2309.1872	0.0037
7	2	2	0	2	1	1	2418.8986	-0.0004
8	8	2	6	8	1	7	2419.8610	-0.0017
9	1	1	1	0	0	0	2664.1793	0.0020
10	2	2	1	2	1	2	2713.5066	-0.0025
11	9	2	7	9	1	8	2734.4615	-0.0249
12	3	2	2	3	1	3	2870.7036	0.0001
13	7	1	6	7	0	7	2879.5373	-0.0035
14	2	0	2	1	1	1	2909.4215	0.0029
15	4	2	3	4	1	4	3082.6590	0.0022
16	10	2	8	10	1	9	3173.2663	-0.0215
17	10	3	7	10	2	8	3251.5794	-0.0121
18	5	2	4	5	1	5	3350.0913	0.0031
19	9	3	6	9	2	7	3359.1402	-0.0011
20	8	1	7	8	0	8	3522.8443	-0.0038
21	8	3	5	8	2	6	3529.3590	0.0029
22	2	1	2	1	1	1	3620.5246	0.0031
23	6	2	5	6	1	6	3672.5534	0.0030
24	2	0	2	1	0	1	3712.7407	0.0053
25	7	3	4	7	2	5	3725.9660	0.0004
26	11	2	9	11	1	10	3729.1998	-0.0145
27	2	1	1	1	1	0	3822.9038	-0.0022
28	6	3	3	6	2	4	3913.9841	-0.0045
29	7	2	6	7	1	7	4047.9767	-0.0010
30	5	3	2	5	2	3	4066.8434	0.0019
31	4	3	1	4	2	2	4171.7908	0.0029
32	9	1	8	9	0	9	4209.9432	0.0114
33	3	3	0	3	2	1	4230.9212	0.0045
34	3	3	1	3	2	2	4274.8018	-0.0030
35	4	3	2	4	2	3	4298.4038	-0.0019
36	4	1	4	3	2	1	4309.3210	-0.0033
37	5	3	3	5	2	4	4344.3314	-0.0043
38	6	3	4	6	2	5	4421.1090	-0.0019
39	2	1	2	1	0	1	4423.8411	0.0028
40	8	2	7	8	1	8	4472.5307	0.0065
41	7	3	5	7	2	6	4536.8531	0.0023
42	8	3	6	8	2	7	4698.5570	0.0063
43	3	0	3	2	1	2	4835.9974	-0.0023
44	12	4	8	12	3	9	4879.2824	0.0212
45	9	3	7	9	2	8	4911.5216	0.0211
46	9	2	8	9	1	9	4940.7421	-0.0045
47	5	2	4	4	3	1	4982.2859	-0.0029
48	11	4	7	11	3	8	5153.0303	-0.0083
49	10	3	8	10	2	9	5178.8713	-0.0003
50	5	2	3	4	3	2	5277.0581	0.0067
51	4	1	3	3	2	2	5362.0912	-0.0001
52	10	4	6	10	3	7	5402.7570	-0.0039
53	3	1	3	2	1	2	5425.3726	-0.0027
54	10	2	9	10	1	10	5446.0710	-0.0175

55	3	0	3	2	0	2	5547.1016	-0.0009
56	3	2	2	2	2	1	5582.5721	0.0024
57	9	4	5	9	3	6	5605.6138	-0.0213
58	3	2	1	2	2	0	5617.9919	0.0048
59	3	1	2	2	1	1	5728.4380	0.0012
60	8	4	4	8	3	5	5753.6991	-0.0037
61	5	1	5	4	2	2	5803.9837	-0.0048
62	7	4	3	7	3	4	5851.5027	-0.0044
63	12	3	10	12	2	11	5877.8331	0.0341
64	6	4	2	6	3	3	5910.3391	0.0058
65	5	4	1	5	3	2	5942.5933	-0.0005
66	7	4	4	7	3	5	5946.9821	-0.0031
67	6	4	3	6	3	4	5950.0257	-0.0015
68	8	4	5	8	3	6	5952.4150	-0.0051
69	5	4	2	5	3	3	5956.1763	-0.0007
70	4	4	0	4	3	1	5958.6060	0.0155
71	4	4	1	4	3	2	5962.0324	-0.0135
72	9	4	6	9	3	7	5973.4478	-0.0108
73	10	4	7	10	3	8	6018.4505	0.0256
74	11	4	8	11	3	9	6096.0541	-0.0020
75	3	1	3	2	0	2	6136.4760	-0.0022
76	12	4	9	12	3	10	6214.6324	-0.0131
77	2	2	1	1	1	0	6232.8330	-0.0020
78	2	2	0	1	1	1	6342.9987	-0.0018
79	13	4	10	13	3	11	6381.2654	0.0174
80	6	2	5	5	3	2	6766.4935	-0.0010
81	4	0	4	3	1	3	6768.1818	0.0010
82	7	3	5	6	4	2	7121.2152	0.0030
83	6	1	6	5	2	3	7160.7814	-0.0043
84	7	3	4	6	4	3	7221.4528	0.0009
85	4	1	4	3	1	3	7224.4154	0.0002
86	8	4	4	7	5	3	7310.3439	-0.0007
87	12	5	7	12	4	8	7314.4913	-0.0025
88	6	2	4	5	3	3	7328.1285	0.0006
89	4	0	4	3	0	3	7357.5563	-0.0001
90	4	2	3	3	2	2	7436.3688	0.0004
91	5	1	4	4	2	3	7438.0041	0.0031
92	4	3	2	3	3	1	7459.9703	0.0009
93	4	3	1	3	3	0	7462.9463	-0.0023
94	4	2	2	3	2	1	7522.0779	0.0004
95	10	5	5	10	4	6	7527.3809	-0.0307
96	9	5	4	9	4	5	7583.9395	-0.0061
97	10	5	6	10	4	7	7588.7883	-0.0152
98	9	5	5	9	4	6	7611.2433	0.0075
99	8	5	3	8	4	4	7620.2877	0.0075
100	4	1	3	3	1	2	7626.1533	0.0001
101	8	5	4	8	4	5	7631.0791	0.0094
102	7	5	2	7	4	3	7643.1898	0.0092
103	7	5	3	7	4	4	7646.8580	0.0060
104	6	5	1	6	4	2	7657.2953	0.0301
105	6	5	2	6	4	3	7658.2673	-0.0146
106	5	5	0	5	4	1	7665.6434	0.0486
107	5	5	1	5	4	2	7665.7499	-0.0504
108	4	1	4	3	0	3	7813.7893	-0.0015
109	3	2	2	2	1	1	7992.4967	-0.0020

^aFrequency. ^bObserved minus calculated frequency according to fit of Table 1.

Table S3. Rotational transitions for the ^{34}S species of DADS.

	J'	K_{-I}'	K_{+I}'	J''	K_{-I}''	K_{+I}''	Freq. ^a (MHz)	o-c ^b (MHz)
1	5	2	3	5	1	4	2081.8881	-0.0019
2	7	2	5	7	1	6	2191.6914	0.0322
3	3	2	1	3	1	2	2245.2838	-0.0048
4	2	2	0	2	1	1	2355.7602	-0.0152
5	1	1	1	0	0	0	2635.5235	-0.0041
6	2	2	1	2	1	2	2654.5146	0.0006
7	3	2	2	3	1	3	2814.3010	-0.0128
8	2	0	2	1	1	1	2915.2407	-0.0022
9	4	2	3	4	1	4	3029.8296	0.0007
10	5	2	4	5	1	5	3301.7162	-0.0189
11	2	1	2	1	1	1	3604.0897	-0.0056
12	2	0	2	1	0	1	3697.3523	0.0003
13	6	3	3	6	2	4	3798.0125	-0.0273
14	2	1	1	1	1	0	3809.5538	-0.0119
15	5	3	2	5	2	3	3955.3030	-0.0179
16	4	3	1	4	2	2	4064.5893	-0.0030
17	3	3	0	3	2	1	4126.6519	0.0146
18	3	3	1	3	2	2	4172.9447	0.0311
19	4	3	2	4	2	3	4197.7855	0.0130
20	5	3	3	5	2	4	4246.0566	-0.0096
21	6	3	4	6	2	5	4326.6321	0.0141
22	2	1	2	1	0	1	4386.1980	-0.0062
23	3	0	3	2	1	2	4833.9855	-0.0029
24	5	2	3	4	3	2	5353.9759	0.0182
25	4	1	3	3	2	2	5399.8497	-0.0004
26	3	1	3	2	1	2	5400.4450	-0.0001
27	3	0	3	2	0	2	5522.8313	-0.0095
28	3	2	1	2	2	0	5597.6025	0.0031
29	3	1	2	2	1	1	5708.0813	-0.0048
30	5	4	1	5	3	2	5797.3376	0.0207
31	6	4	3	6	3	4	5806.1848	0.0174
32	5	1	5	4	2	2	5807.1488	0.0279
33	4	4	0	4	3	1	5814.4229	-0.0077
34	4	4	1	4	3	2	5818.2255	0.0019
35	3	1	3	2	0	2	6089.2953	-0.0021
36	2	2	1	1	1	0	6155.8663	-0.0046
37	2	2	0	1	1	1	6268.0696	-0.0100
38	4	0	4	3	1	3	6756.8629	-0.0015
39	4	1	4	3	1	3	7190.6890	-0.0069
40	4	0	4	3	0	3	7323.3148	-0.0063
41	5	1	4	4	2	3	7469.8250	-0.0151
42	4	2	2	3	2	1	7496.3942	0.0084
43	4	1	3	3	1	2	7598.3211	0.0069
44	4	1	4	3	0	3	7757.1513	-0.0013
45	3	2	2	2	1	1	7906.5448	-0.0053

^aFrequency. ^bObserved minus calculated frequency according to fit of Table 1.

Table S4. Rotational transitions for the ${}^34\text{S}'$ species of DADS.

	J'	K_{-I}'	K_{+I}'	J''	K_{-I}''	K_{+I}''	Freq. ^a (MHz)	o-c ^b (MHz)
1	4	2	2	4	1	3	2149.1175	0.0097
2	3	2	1	3	1	2	2250.8551	0.0001
3	2	2	0	2	1	1	2359.6198	0.0127
4	1	1	1	0	0	0	2636.4400	-0.0033
5	2	2	1	2	1	2	2651.0323	0.0000
6	3	2	2	3	1	3	2806.6607	-0.0009
7	2	0	2	1	1	1	2913.2420	-0.0008
8	2	1	2	1	1	1	3605.6693	0.0166
9	2	0	2	1	0	1	3696.7804	-0.0061
10	2	1	1	1	1	0	3805.9294	-0.0028
11	5	3	2	5	2	3	3965.3355	-0.0207
12	4	3	1	4	2	2	4070.1335	0.0030
13	3	3	0	3	2	1	4129.3174	0.0000
14	3	3	1	3	2	2	4173.3090	-0.0126
15	4	3	2	4	2	3	4196.9758	-0.0015
16	5	3	3	5	2	4	4242.9694	-0.0163
17	6	3	4	6	2	5	4319.8216	-0.0127
18	2	1	2	1	0	1	4389.1928	-0.0034
19	3	0	3	2	1	2	4830.7209	0.0067
20	4	1	3	3	2	2	5385.7909	0.0109
21	3	1	3	2	1	2	5403.0621	0.0037
22	3	0	3	2	0	2	5523.1200	-0.0038
23	3	2	2	2	2	1	5558.6928	0.0049
24	3	2	1	2	2	0	5594.2034	0.0014
25	3	1	2	2	1	1	5702.9625	0.0083
26	7	4	3	7	3	4	5708.4151	-0.0257
27	6	4	2	6	3	3	5767.7510	-0.0133
28	5	4	1	5	3	2	5800.3165	0.0209
29	7	4	4	7	3	5	5805.3471	0.0253
30	5	4	2	5	3	3	5814.1172	0.0172
31	3	1	3	2	0	2	6095.4664	-0.0018
32	2	2	1	1	1	0	6156.5321	-0.0096
33	2	2	0	1	1	1	6265.6730	-0.0095
34	4	0	4	3	1	3	6753.2104	0.0043
35	4	1	4	3	1	3	7194.6487	0.0041
36	7	3	5	6	4	2	7207.2274	0.0011
37	4	0	4	3	0	3	7325.5580	0.0074
38	10	5	6	10	4	7	7406.4760	0.0234
39	4	3	2	3	3	1	7428.1364	-0.0233
40	4	3	1	3	3	0	7431.1762	-0.0128
41	4	1	4	3	0	3	7766.9976	0.0087
42	3	2	2	2	1	1	7909.2873	-0.0099

^aFrequency. ^bObserved minus calculated frequency according to fit of Table 1.

Table S5. Rotational transitions for the $^{13}\text{C}(1)$ species of DADS.

	J'	K_{-I}'	K_{+I}'	J''	K_{-I}''	K_{+I}''	Freq. ^a (MHz)	o-c ^b (MHz)
1	2	1	2	1	0	1	4401.1708	0.0038
2	3	0	3	2	1	2	4785.1143	0.0015
3	3	1	3	2	0	2	6101.5571	0.0120
4	2	2	1	1	1	0	6217.2029	-0.0121
5	2	2	0	1	1	1	6324.9665	-0.0183
6	2	2	1	2	1	2	2724.0940	0.0076
7	2	0	2	1	1	1	2874.1161	0.0257
8	2	0	2	1	0	1	3682.9400	0.0068
9	2	1	1	1	1	0	3790.7074	-0.0006
10	4	3	1	4	2	2	4198.4924	0.0080
11	3	3	1	3	2	2	4297.1971	-0.0051
12	4	3	2	4	2	3	4319.8207	0.0240
13	5	3	3	5	2	4	4363.8111	-0.0034
14	4	1	3	3	2	2	5279.2900	0.0072
15	3	1	3	2	1	2	5383.2718	-0.0395
16	3	0	3	2	0	2	5503.3789	0.0324
17	3	2	1	2	2	0	5571.1289	-0.0211
18	3	1	2	2	1	1	5680.3941	-0.0119
19	4	0	4	3	1	3	6702.5747	0.0043
20	4	1	4	3	1	3	7168.7233	0.0053
21	4	0	4	3	0	3	7300.7731	0.0042
22	3	2	2	2	1	1	7963.7751	-0.0051

^aFrequency. ^bObserved minus calculated frequency according to fit of Table 1.

Table S6. Rotational transitions for the $^{13}\text{C}(2)$ species of DADS.

	J'	K_{-I}'	K_{+I}'	J''	K_{-I}''	K_{+I}''	Freq. ^a (MHz)	o-c ^b (MHz)
1	1	1	1	0	0	0	2647.9000	-0.0191
2	2	0	2	1	1	1	2879.8543	0.0069
3	2	0	2	1	0	1	3682.1994	0.0300
4	2	1	1	1	1	0	3792.5762	0.0267
5	3	1	0	3	2	1	4226.2150	0.0145
6	3	3	1	3	2	2	4270.2653	-0.0133
7	4	3	2	4	2	3	4293.9912	0.0112
8	5	3	3	5	2	4	4340.1032	0.0034
9	2	1	2	1	0	1	4392.1506	0.0035
10	3	0	3	2	1	2	4791.1646	-0.0165
11	3	1	3	2	1	2	5379.3191	0.0114
12	3	0	3	2	0	2	5501.1479	-0.0110
13	2	2	1	1	1	0	6199.4812	-0.0128
14	2	2	0	1	1	1	6309.8476	-0.0214
15	4	0	4	3	1	3	6707.9893	-0.0291
16	4	1	3	3	1	2	7565.3746	0.0251
17	4	1	4	3	0	3	7751.0839	0.0043

^aFrequency. ^bObserved minus calculated frequency according to fit of Table 1.

Table S7. Rotational transitions for the $^{13}\text{C}(3)$ species of DADS.

	J'	K_{-I}'	K_{+I}'	J''	K_{-I}''	K_{+I}''	Freq. ^a (MHz)	o-c ^b (MHz)
1	1	1	1	0	0	0	2630.2363	0.0099
2	3	2	2	3	1	3	2846.6452	0.0253
3	2	0	2	1	1	1	2871.5572	0.0051
4	3	2	2	3	1	3	2846.6452	0.0253
5	2	1	2	1	1	1	3571.5038	-0.0141
6	2	0	2	1	0	1	3664.7313	-0.0114
7	3	3	0	3	2	1	4182.2338	0.0070
8	3	3	1	3	2	2	4227.7363	-0.0236
9	4	3	2	4	2	3	4252.2133	-0.0158
10	2	1	2	1	0	1	4364.7114	0.0028
11	3	0	3	2	1	2	4774.3302	0.0006
12	3	1	3	2	1	2	5351.6822	0.0126
13	3	0	3	2	0	2	5474.2914	-0.0039
14	3	1	2	2	1	1	5658.7908	0.0287
15	3	1	3	2	0	2	6051.6475	0.0121
16	2	2	1	1	1	0	6156.1514	-0.0101
17	4	0	4	3	1	3	6681.8295	0.0066
18	4	1	4	3	0	3	7703.1650	0.0165
19	3	2	2	2	1	1	7890.6485	0.0022
20	3	2	1	3	1	2	2277.9499	0.0012
21	4	2	2	3	2	1	7429.6101	0.0059
22	3	2	1	2	2	0	5547.8114	-0.0354
23	4	1	3	3	1	2	7532.7434	-0.0303

^aFrequency. ^bObserved minus calculated frequency according to fit of Table 1.

Table S8. Rotational transitions for the $^{13}\text{C}(1')$ species of DADS.

	J'	K_{-I}'	K_{+I}'	J''	K_{-I}''	K_{+I}''	Freq. ^a (MHz)	o-c ^b (MHz)
1	1	1	1	0	0	0	2653.2625	0.0048
2	2	2	1	2	1	2	2701.2130	-0.0422
3	2	0	2	1	1	1	2894.7131	-0.0030
4	4	2	3	4	1	4	3063.6632	0.0107
5	2	0	2	1	0	1	3695.7511	0.0025
6	2	1	1	1	1	0	3803.8512	0.0154
7	3	3	0	3	2	1	4216.2264	0.0324
8	3	3	1	3	2	2	4258.7265	0.0114
9	4	3	2	4	2	3	4281.5515	-0.0390
10	2	1	2	1	0	1	4406.0750	-0.0086
11	3	0	3	2	1	2	4811.9500	-0.0185
12	3	0	3	2	0	2	5522.2898	-0.0138
13	3	2	1	2	2	0	5590.9773	0.0019
14	3	1	3	2	0	2	6112.6750	0.0026
15	2	2	1	1	1	0	6206.9250	0.0138
16	2	2	0	1	1	1	6315.0000	0.0066
17	4	0	4	3	1	3	6735.2685	0.0124
18	4	1	4	3	1	3	7193.9784	-0.0008
19	4	1	4	3	0	3	7784.3413	-0.0065
20	3	2	2	2	1	1	7959.7414	0.0015

^aFrequency. ^bObserved minus calculated frequency according to fit of Table 1.

Table S9. Rotational transitions for the $^{13}\text{C}(2')$ species of DADS.

	J'	K_{-I}'	K_{+I}'	J''	K_{-I}''	K_{+I}''	Freq. ^a (MHz)	o-c ^b (MHz)
1	4	2	2	4	1	3	2234.0052	-0.0146
2	3	2	1	3	1	2	2338.7707	-0.0007
3	2	2	0	2	1	1	2448.2990	-0.0173
4	1	1	1	0	0	0	2652.8357	-0.0020
5	4	2	3	4	1	4	3099.6193	-0.0153
6	2	1	2	1	1	1	3579.8525	0.0230
7	2	0	2	1	0	1	3670.5499	-0.0347
8	3	3	0	3	2	1	4277.7070	-0.0080
9	2	1	2	1	0	1	4393.0985	0.0068
10	3	0	3	2	1	2	4762.3764	0.0061
11	3	1	3	2	1	2	5364.5903	0.0076
12	3	0	3	2	0	2	5484.8806	0.0033
13	3	2	2	2	2	1	5518.7203	0.0049
14	3	1	2	2	1	1	5662.0633	0.0147
15	4	4	0	4	3	1	6022.5861	0.0404
16	3	1	3	2	0	2	6087.0961	0.0064
17	2	2	0	1	1	1	6326.0847	-0.0085
18	4	0	4	3	1	3	6674.0317	0.0226
19	4	1	4	3	1	3	7143.7523	-0.0146
20	4	0	4	3	0	3	7276.1944	-0.0270
21	4	1	4	3	0	3	7745.9909	0.0116
22	3	2	2	2	1	1	7958.4568	-0.0236

^aFrequency. ^bObserved minus calculated frequency according to fit of Table 1.

Table S10. Rotational transitions for the $^{13}\text{C}(3')$ species of DADS.

	J'	K_{-I}'	K_{+I}'	J''	K_{-I}''	K_{+I}''	Freq. ^a (MHz)	o-c ^b (MHz)
1	1	1	1	0	0	0	2634.3879	-0.0076
2	2	0	2	1	1	1	2860.0131	-0.0133
3	4	2	3	4	1	4	3056.1757	0.0138
4	2	1	2	1	1	1	3569.9885	0.0318
5	2	0	2	1	0	1	3660.1011	0.0190
6	2	1	1	1	1	0	3767.4012	0.0122
7	2	1	2	1	0	1	4370.0140	0.0016
8	3	0	3	2	1	2	4759.1268	0.0019
9	3	1	3	2	1	2	5349.7647	0.0079
10	3	0	3	2	0	2	5469.0398	-0.0153
11	3	2	2	2	2	1	5502.9898	-0.0185
12	3	1	2	2	1	1	5645.4399	0.0193
13	3	1	3	2	0	2	6059.6901	0.0031
14	2	2	1	1	1	0	6167.5277	-0.0065
15	2	2	0	1	1	1	6274.8278	-0.0082
16	4	0	4	3	1	3	6664.4155	0.0018
17	4	0	4	3	0	3	7255.0659	0.0204
18	4	3	2	3	3	1	7353.1910	-0.0062
19	4	2	2	3	2	1	7412.7410	0.0118
20	4	1	3	3	1	2	7515.9536	-0.0392
21	4	1	4	3	0	3	7714.6037	-0.0039
22	3	2	2	2	1	1	7903.1538	0.0001

^aFrequency. ^bObserved minus calculated frequency according to fit of Table 1.

Table S11. Rotational constants for the isotopic species of DADS.

	Isotopologues							
	³⁴ S	³⁴ S'	¹³ C(1)	¹³ C(2)	¹³ C(3)	¹³ C(1')	¹³ C(2')	¹³ C(3')
<i>A</i> / MHz ^a	1760.18891(73) ^c	1760.06647(68)	1781.3226(15)	1775.8047(19)	1762.9848(17)	1776.8440(17)	1782.7103(18)	1766.5866(25)
<i>B</i> / MHz	978.08036(52)	976.52317(72)	972.4801(13)	973.4830(21)	969.7945(14)	975.8121(18)	969.4485(17)	966.5314(12)
<i>C</i> / MHz	875.34086(49)	876.37902(63)	873.2838(12)	872.1165(17)	867.2436(11)	876.4156(11)	870.1294(11)	867.8109(10)
<i>D_J</i> / kHz				[0.6173] ^d				
<i>D_{JK}</i> / kHz				[-1.9591]				
<i>D_K</i> / kHz				[4.050]				
<i>d₁</i> / kHz				[-0.13453]				
<i>d₂</i> / kHz				[-0.00959]				
<i>N</i> ^b	45	42	22	17	23	20	22	22
σ / kHz	12.8	11.8	15.7	17.5	16.7	17.3	17.6	15.4

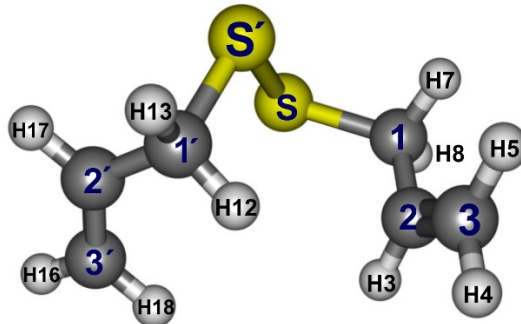
^aRotational constants (*A*, *B*, *C*) and Watson's S-reduction centrifugal distortion constants (*D_J*, *D_{JK}*, *D_K*, *d₁*, *d₂*) ^bNumber of transitions (*N*) and rms deviation (σ) of the fit.

^cStandard error in units of the last digit. ^dParameters in square brackets were kept fixed in the fit.

Table S12. Core correlation for the bond lengths (in Å) in dimethyl disulfide.

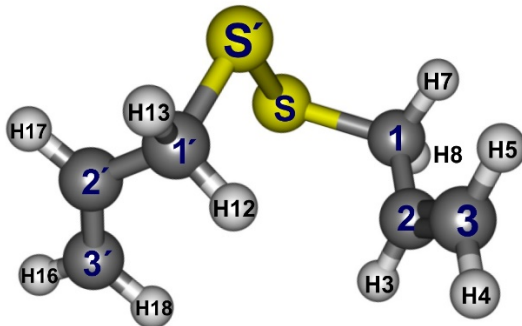
	$r(\text{S-S})$	$r(\text{C-S})$	$r(\text{C-H})$
CCSD(T)/wCVQZ	-0.0054	-0.0046	-0.0015
MP2/wCVTZ	-0.0056	-0.0047	-0.0014

Table S13. Full structure of DADS (bond lengths in Å and angles in degrees).



Parameter	r_e^{BO}	Predicate	$r_m^{(1)}$	Parameter	r_e^{BO}	Predicate	$r_m^{(1)}$
C2C3	1.3341	1.3337	1.3337(15)	C1SS'	102.5641	102.19	102.284(92)
C2H3	1.0845	1.0843	1.0844(13)	SS'C1'	103.4401	102.97	103.910(35)
C2C1	1.4891	1.4870	1.4870(14)	S'C1'C2'	112.2558	111.72	112.24(15)
C3H4	1.0809	1.0806	1.0806(13)	H12C1'C2'	111.9389	112.04	112.02(26)
C3H5	1.0821	1.0814	1.0814(13)	H13C1'C2'	111.6182	111.90	111.91(26)
C1H7	1.0882	1.0886	1.0886(13)	C2'C3'H16	121.4445	121.37	121.44(26)
C1H8	1.0921	1.0923	1.0923(13)	C2'C3'H18	121.0259	120.82	120.89(26)
C1S	1.8298	1.8314	1.8325(10)	C1'C2'C3'	123.2486	123.05	123.268(51)
SS'	2.0328	2.0275	2.0282(13)	C3'C2'H17	120.1259	120.01	120.00(26)
S'C1'	1.8322	1.8334	1.8332(15)	H4C3C2C1	179.2387	179.18	179.27(60)
C1'H12	1.0871	1.0874	1.0874(13)	C1C2C3H5	-0.907	-1.10	-1.14(61)
C1'H13	1.0921	1.0923	1.0923(13)	SC1C2C3	-113.2476	-112.58	-114.43(14)
C1'C2'	1.4883	1.486	1.4851(16)	H3C2C1S	65.1092	65.77	67.79(60)
C3'C2'	1.3336	1.3330	1.3314(12)	S'SC1C2	67.7303	67.29	68.93(27)
C3'H16	1.0806	1.0803	1.0803(13)	H7C1SS'	-56.3939	-57.06	-56.94(58)
C3'H18	1.0823	1.0815	1.0816(13)	H8C1SS'	-171.6627	-172.11	-172.27(58)
C2'H17	1.0837	1.0836	1.0836(13)	C1SS'C1'	-92.9469	-93.80	-93.63(14)
C3C2C1	123.3974	123.18	123.50(16)	SS'C1'C2'	-64.41	-64.47	-63.44(16)
H3C2C1	116.4789	116.79	116.81(26)	S'C1'C2'C3'	113.0231	112.50	115.05(24)
C2C3H4	121.4126	121.33	121.29(26)	H12C1'C2'C3'	-9.5576	-10.16	-10.02(61)
C2C3H5	121.0279	120.82	120.80(26)	H13C1'C2'C3'	-131.8041	-132.66	-132.79(60)
C2C1S	113.0249	112.60	112.92(10)	H16C3'C2'C1'	-178.7367	-178.61	-178.69(60)
H7C1S	108.4912	108.52	108.52(26)	H18C3'C2'C1'	1.2394	1.51	0.67(60)
H8C1S	103.3326	103.35	103.37(26)	H17C2'C3'C1'	177.638	177.49	177.44(61)

Table S14. Different computational structures of DADS (bond lengths in Å and angles in degrees).



Method Basis set	CCSD(T)_FC V(T+d)Z	MP2(AE) wCVTZ	MP2(FC) wCVTZ	MP2(FC) V(Q+d)Z	MP2(FC) V(T+d)Z	r_e^{BO} ^a
C2C3	1.3392	1.3319	1.3347	1.3343	1.3365	1.3341
C2H3	1.0864	1.0829	1.0842	1.0837	1.0843	1.0845
H3C2C3	120.095	119.970	119.982	120.021	120.001	120.103
C3H4	1.0831	1.0790	1.0803	1.0797	1.0806	1.0809
H4C3C2	121.422	121.346	121.335	121.310	121.331	121.413
H4C3C2H3	0.910	0.960	0.970	1.030	0.991	0.939
C3H5	1.0842	1.0799	1.0812	1.0807	1.0814	1.0821
H5C3C2	121.023	120.854	120.851	120.824	120.821	121.028
H5C3C2H3	-179.231	-179.322	-179.310	-179.263	-179.300	-179.207
C1C2	1.4948	1.4810	1.4842	1.4833	1.4857	1.4891
C1C2C3	123.404	123.242	123.217	123.147	123.179	123.397
C1C2C3H3	178.398	177.881	177.901	177.804	177.882	178.300
C1H7	1.0903	1.0868	1.0882	1.0879	1.0886	1.0882
H7C1C2	111.369	111.484	111.467	111.519	111.461	111.444
H7C1C2C3	9.251	11.472	11.352	11.220	11.347	9.244
C1H8	1.0943	1.0904	1.0919	1.0914	1.0923	1.0921
H8C1C2	111.351	111.760	111.746	111.833	111.742	111.454
H8C1C2C3	130.771	133.403	133.303	133.327	133.310	130.888
C1S	1.8388	1.8246	1.8293	1.8270	1.8314	1.8298
SC1C2	113.120	112.576	112.604	112.533	112.600	113.025
SC1C2C3	-113.325	-110.786	-110.900	-110.925	-110.888	-113.248
SS'	2.0474	2.0194	2.0250	2.0186	2.0275	2.0328
S'SC1	102.437	102.248	102.262	102.334	102.193	102.564
S'SC1C2	68.085	65.803	65.867	65.566	65.857	67.730
S'C1'	1.8412	1.8266	1.8313	1.8291	1.8334	1.8322
C1'S'S	103.315	103.024	103.046	103.115	102.967	103.440
C1'S'SC1	-92.928	-93.837	-93.720	-93.631	-93.730	-92.947
C1'H12	1.0891	1.0856	1.0870	1.0868	1.0874	1.0871
H12C1'S'	108.750	108.667	108.659	108.595	108.642	108.710
H12C1'S'S	59.723	60.802	60.730	60.840	60.656	59.979
C1'H13	1.0944	1.0905	1.0919	1.0915	1.0923	1.0921
H13C1'S'	103.099	103.179	103.152	103.121	103.160	103.087
H13C1'S'S	175.096	176.303	176.245	176.367	176.184	175.337

C1'C3'	2.4933	2.4732	2.4781	2.4763	2.4807	2.4839
C3'C1'S'	120.233	118.471	118.567	118.462	118.538	120.062
C3'C1'S'S	-36.156	-34.629	-34.685	-34.498	-34.709	-35.890
C2'C3'	1.3386	1.3311	1.3339	1.3336	1.3358	1.3336
C2'C3'C1'	30.074	30.086	30.101	30.129	30.116	30.072
C2'C3'C1'S'	-79.751	-81.863	-81.770	-81.795	-81.847	-79.793
C3'H16	1.0828	1.0786	1.0800	1.0794	1.0803	1.0806
H16C3'C1'	151.526	151.440	151.448	151.442	151.457	151.504
H16C3'C1'S'	-77.686	-78.709	-78.684	-78.575	-78.752	-77.533
C2'H17	1.0857	1.0822	1.0835	1.0830	1.0836	1.0837
H17C2'C3'	120.136	119.977	119.990	120.016	120.012	120.126
H17C2'C3'C1'	177.753	177.017	177.049	176.934	177.017	177.638
C13'H18	1.0843	1.0800	1.0813	1.0808	1.0815	1.0823
H18C3'C1'	90.942	90.783	90.763	90.716	90.718	90.960
H18C3'C1'S'	101.224	99.773	99.832	99.873	99.767	101.270

^a $r_e^{BO} = \text{CCSD(T)}_{\text{FC}}/\text{V}(\text{T+d})\text{Z} + \text{MP2}/[\text{V}(\text{Q+d})\text{Z}(\text{FC}) - \text{V}(\text{T+d})\text{Z}(\text{FC}) + w\text{CVTZ(AE)} - w\text{CVTZ(FC)}]$

Table S15. A comparison of the Kraitchman's substitution structure for DADS and the equilibrium structure.

Parameter	r_s	r_e^{BO}	$r_m^{(1)}$
C2C3	1.3300(40)	1.3341	1.3337(15)
C2C1	1.4988(44)	1.4891	1.4870(14)
C1S	1.8428(40)	1.8298	1.8325(10)
SS'	2.0234(30)	2.0328	2.0282(13)
S'C1'	1.8184(32)	1.8322	1.8332(15)
C1'C2'	1.4903(159)	1.4883	1.4851(16)
C3'C2'	1.3292(198)	1.3336	1.3314(12)
C3C2C1	123.86(25)	123.3974	123.50(16)
C2C1S	112.75(17)	113.0249	112.92(10)
C1SS'	102.68(15)	102.5641	102.284(92)
SS'C1'	103.90(11)	103.4401	103.910(35)
S'C1'C2'	112.48(28)	112.2558	112.24(15)
C1'C2'C3'	123.72(30)	123.2486	123.268(51)
SC1C2C3	-114.48(15)	-113.2476	-114.43(14)
S'SC1C2	68.44(25)	67.7303	68.93(27)
C1SS'C1'	-93.61(20)	-92.9469	-93.63(14)
SS'C1'C2'	-63.228(72)	-64.41	-63.44(16)
S'C1'C2'C3'	114.325(68)	113.0231	115.05(24)

Table S16. Natural-Bond-Orbital (NBO) analysis of conformer 1 (C_1) of DADS using B3LYP-GD3(BJ)/6-311++G(d,p). List of most important hyperconjugative interactions according to a second-order perturbation theory analysis of the Fock matrix in the NBO basis (bond orders or lone-pairs in parentheses).

Donor NBO	Acceptor NBO	$E(2)$ / kJ mol ⁻¹
BD(2) C3'-C2'	BD*(1) S'-C1'	25.1
BD(1) C3-H4	BD*(1) C2-C1	24.9
BD(1) C3'-H16	BD*(1) C1'-C2'	24.6
BD(2) C2-C3	BD*(1) C1-S	24.0
LP(2) S	BD*(1) S'-C1'	23.0
BD(1) C3-H5	BD*(1) C2-H3	22.8
BD(1) C3'-H18	BD*(1) C2'-H17	22.4
LP(2) S'	BD*(1) C1-S	21.3
BD(1) C2-H3	BD*(1) C2-H5	19.6
BD(1) C2'-H17	BD*(1) C3'-H18	19.6
BD(1) C1-S	BD*(2) C2-C3	18.6
BD(1) S'-C1'	BD*(2) C3'-C2'	18.6

Table S17. Natural-Bond-Orbital (NBO) analysis of conformer 2 (C_2) of DADS using B3LYP-GD3(BJ)/6-311++G(d,p). List of most important hyperconjugative interactions according to a second-order perturbation theory analysis of the Fock matrix in the NBO basis (bond orders or lone-pairs in parentheses).

Donor NBO	Acceptor NBO	$E(2)$ / kJ mol ⁻¹
BD(1) C3-H4	BD*(1) C2-C1	25.4
BD(1) C3'-H16	BD*(1) C1'-C2'	25.4
LP(2) S	BD*(1) S'-C1'	24.1
LP(2) S'	BD*(1) C1-S	24.1
BD(2) C2-C3	BD*(1) C1-S	24.0
BD(2) C3'-C2'	BD*(1) S'-C1'	24.0
BD(1) C3-H5	BD*(1) C2-H3	22.4
BD(1) C3'-H18	BD*(1) C2'-H17	22.4
BD(1) C2-H3	BD*(1) C3-H5	19.9
BD(1) C2'-H17	BD*(1) C3'-H18	19.9
BD(1) C1-S	BD*(2) C2-C3	17.3
BD(1) S'-C1'	BD*(2) C3'-C2'	17.3

Table S18. Selection of bond lengths (\AA) for the double bond C=C.

	r_e	MP2/VTZ	$r_e - \text{calc.}$	Ref.
H2C=C=CH2	1.3074	1.3082	-0.0008	1
H2C=C=O	1.3122	1.3161	-0.0039	2
CH2=CF2	1.3181	1.3213	-0.0032	3
CH2=CHF	1.3210	1.3240	-0.0030	4
CHF=CHF trans	1.3239	1.3257	-0.0018	5
CHCl=CHF trans	1.3240	1.3281	-0.0041	6
CHF=CHF cis	1.3246	1.3264	-0.0018	7
CHCl=CHF cis	1.3249	1.3288	-0.0039	8
CH2=CHBr	1.3256	1.3289	-0.0033	9
CH2=CHCl	1.3262	1.3289	-0.0027	10
CH2=CHI	1.3276	1.3306	-0.0030	11
H2C=C=C:	1.3283	1.3316	-0.0033	12
CHF=CH-CH=CHF	1.3296	1.3337	-0.0041	13
CHF=CH-CH=CHF	1.3300	1.3333	-0.0033	14
CH2=CHOH	1.3303	1.3334	-0.0031	15
CH2=CH2	1.3315	1.3319	-0.0012	16
CH2=CHCH3	1.3317	1.3338	-0.0021	17
CH2=CHCHO	1.3348	1.3375	-0.0027	18
H2C=CHCN	1.3352	1.3374	-0.0022	19
H2C=CHNH2	1.3357	1.3379	-0.0022	20
C2H2(CO)2O	1.3325	1.3358	<u>-0.0033</u>	21
Median			-0.0030	
Mean			-0.0028	
maximum			-0.0008	
Minimum			-0.0041	

- [1] A. A. Auer, J. Gauss PCCP 2001, 3, 3001-3005. [2] A. Guarnieri, J. Demaison, H. D. Rudolph J. Mol. Struct. 2010, 969, 1-8. [3] D. Feller, N. C. Craig, P. Groner, D. C. McKean J. Phys. Chem. A 2011, 115, 94-98. [4] J. Demaison J. Mol. Spectrosc. 2006, 239, 201-207. [5] See 3. [6] C. Puzzarini, G. Cazzoli, A. Gambi, J. Gauss J. Chem. Phys. 2006, 125, 054307. [7] See 3. [8] See 6. [9] N. Zvereva-Loëte, J. Demaison, H. D. Rudolph J. Mol. Spectrosc. 2006, 236, 248-254. [10] J. Demaison, H. Møllendal, A. Perrin, J. Orphal, F. Kwabia Tchana, H. D. Rudolph, F. Willaert J. Mol. Spectrosc. 2005, 232, 174-185. [11] J. Demaison J. Mol. Spectrosc. 2006, 239, 201-207. [12] J. Gauss, J. F. Stanton J. Mol. Struct. 1999, 485-486, 43-50. [13] Demaison, J.; Craig, N. C. J. Phys. Chem. A 2011, 115, 8049–8054. [14] Demaison, J.; Craig, N. C. J. Phys. Chem. A 2011, 115, 8049–8055. [15] J. Demaison, M. Herman, J. Liévin Intern. Rev. Phys. Chem. 2007, 26, 391-420. [16] C. Puzzarini, M. Heckert, J. Gauss, J. Chem. Phys. 128 (2008) 194108/1-9. [17] J. Demaison, N. C. Craig, R. Gurusinghe, M. J. Tubergen, H. D. Rudolph, L. H. Coudert, P. Szalay, A. G. Császár J. Phys. Chem. A 2017, 121, 3155-3166. [18] C. Puzzarini, E. Penocchio, M. Biczysko, V. Barone J. Phys. Chem. A 2014, 118, 6648-6656. [19] E. Askeland, H. Møllendal, E. Uggerud, J.-C. Guillemin, J.-R. Aviles Roreno, J. Demaison, T. R. Huet J. Phys. Chem. A 2006, 110, 12572-12584. [20] See 19. [21] N. Vogt, J. Demaison, H. D. Rudolph Struct. Chem. 2011, 22, 337-343